Journal of Environmental Chemical Engineering 11 (2023) 109803

Contents lists available at ScienceDirect

Journal of Environmental Chemical Engineering

journal homepage: www.elsevier.com/locate/jece

Removal of emerging pollutants from water using enzyme-immobilized activated carbon from coconut shell

Osamah J. Al-sareji [a,b,*], Mónika Meiczinger [a], Viola Somogyi [a], Raed A. Al-Juboori [c,d], Ruqayah Ali Grmasha [b,e], Csilla Stenger-Kovács [e,f], Miklós Jakab [g], Khalid S. Hashim [h,i]

[a] Sustainability Solutions Research Lab, Faculty of Engineering, University of Pannonia, Egyetem str. 10, Veszprém H 8200, Hungary
[b] Environmental Research and Studies Center, University of Babylon, Babylon, Al-Hillah, Iraq
[c] NYUAD Water Research Center, New York University-Abu Dhabi Campus, P.O. Box 129188, Abu Dhabi, United Arab Emirates
[d] Water and Environmental Engineering Research Group, Department of Built Environment, Aalto University, P.O. Box 15200, Aalto, FI-00076 Espoo, Finland
[e] University of Pannonia, Faculty of Engineering, Center for Natural Science, Research Group of Limnology, Egyetem u. 10, H-8200 Veszprem, Hungary
[f] ELKH-PE Limnoecology Research Group, Egyetem utca 10., H-8200 Veszprém, Hungary
[g] Research Centre of Engineering Sciences, Department of Materials Sciences and Engineering, University of Pannonia, P.O. Box 158, H-8201 Veszprém, Hungary
[h] School of Civil Engineering and Built Environment, Liverpool John Moores University, UK
[i] Department of Environmental Engineering, College of Engineering, University of Babylon, Babylon, Al-Hillah, Iraq

ARTICLE INFO

Editor: Yang Liu

Keywords:
Coconut shell biochar
Laccase
Emerging contaminants
Pharmaceutical removal
Adsorption
Enzymatic degradation

ABSTRACT

This work reports the removal of diclofenac, amoxicillin, carbamazepine, and ciprofloxacin by utilizing three commercially available granular activated carbons (GACs) (Activated carbon, Silcarbon, and Donau) loaded with laccase. Adsorption was used to successfully immobilize laccase on the GACs, as revealed by scanning electron microscopy and energy dispersive X-ray analysis (SEM-EDX) and Fourier transform infrared spectroscopy (FTIR). In the three types of GACs tested, pH 5, 30 °C, and 2 mg mL^{-1} laccase content were found to be the optimum immobilization parameters. Laccase immobilization yields of 65.2%, 63.1%, and 62.9% were achieved with activated carbon, Silcarbon, and Donau respectively. The adsorption behaviors of the pharmaceuticals onto the tested activated carbons are best described as a spontaneous endothermic process that follows Langmuir isotherm and first-order kinetics. The reusability of the immobilized enzyme was evaluated using 2, 2′-azino-bis 3-ethylbenzothiazole-6-sulphonic acid (ABTS) as a substrate within six cycles for all adsorbents. In 120 mins, nearly a complete removal of the pharmaceutical compounds (50 mg L^{-1}) was obtained in the case of activated carbon type and more than 90% for other adsorbent types when synergistic adsorption and enzymatic degradation were applied. With adsorption alone, 74% removal was obtained with activated carbon and < 56% for other adsorbents. The finding of this study suggests that biochar produced from coconut shell (same as the one used in this study) can effectively be used as a substrate and adsorbent for pharmaceutical removal. This enzymatic physical removal system has the potential to be applied on a large-scale.

1. Introduction

In recent years, environmental problems posed by emerging contaminants such as pharmaceuticals, microplastics, polycyclic aromatic hydrocarbons, and others have attracted worldwide attention, with a particular emphasis on pharmaceutical contaminants [28]. Generally, some pharmacological substances have hydrophilic properties, while others possess hydrophobic nature. On the one hand, these pharmacokinetic characteristics are regarded as advantageous features for extending the drug's half-life in the human body. On the other hand, these characteristics contribute to the enhanced persistence of these contaminants in the environment [27]. In addition to their characteristics, the unrestricted release of pharmaceutical pollutants from several sources, such as hospitals, domestic disposal, livestock farming, different scientific activities, and others, is significantly faster than their remediation/auto-degradation processes [39]. As a result, pharmaceutical residues accumulate from the ng/L to μg/L range in water matrices [47]. This negatively affects human health, aquatic life, and the development of antimicrobial-resistant microorganisms [17].

Increasing environmental contamination has resulted in a rise in the

* Corresponding author at: Sustainability Solutions Research Lab, Faculty of Engineering, University of Pannonia, Egyetem str. 10, Veszprém H 8200, Hungary.
E-mail address: osamah.al-sareji@unswalumni.com (O.J. Al-sareji).

https://doi.org/10.1016/j.jece.2023.109803
Received 11 January 2023; Received in revised form 22 February 2023; Accepted 27 March 2023
Available online 30 March 2023

types and doses of these pollutants in water bodies. This decreases the quality of water in addition to the many adverse consequences and threats that these toxins represent to the environment and life in general since most of them are mutagenic and carcinogenic. The inadequacy of current wastewater treatment techniques to completely degrade these compounds increases the danger they represent. Further difficulties of techniques such as ozonation, photocatalysis, filtration, and coagulation include high energy consumption, toxic byproducts, and secondary disposal issues [32,44]. Thus, the degradation of these emerging contaminants necessitated the creation of new technologies along with low-cost materials.

Enzymatic degradation is one of the most common methods for removing pharmaceutical chemicals due to its high oxidative capacity at mild reaction parameters with lower energy usage, which renders it significantly safer and more energy-efficient [52]. Nevertheless, certain limitations of free laccase prevent its use in wastewater treatment, including temperature and pH instability, weak reusability, and inactivation [40]. Due to its great effectiveness and low cost, enzyme immobilization is regarded as one of the most promising strategies for overcoming these restrictions. Carriers serve a crucial role in enzyme immobilization. Commonly, inorganic and chemically inert polymers are used as carrier matrices [42].

Since enzyme immobilization can be a physical or chemical method, the characteristics of carriers could have a significant effect on enzyme recovered activity, yield, thermal or operational stability, etc. In addition to cost, other factors, such as pH stability, mechanical strength, reusability, the ability to enhance enzyme thermal, and non-pollution, should be taken into account when selecting carriers. As a result, inorganic and porous materials, such as activated carbon, celite, and biomass are commonly utilized as carriers for the immobilization process [23].

In 2020, the coconut harvest exceeded 61.52 million tons worldwide [35]. This production consists mostly of coconut shell waste. Biochar produced from coconut shell has proven to be a potent adsorbent for water and air purification applications. Coconut shell biochar has a large surface area and porous structure that can be harnessed for carrying enzymes [26]. According to the literature, there were extensive investigations into coconut waste as a carrier for enzyme immobilization, especially coconut fiber because of its composition of hemicellulose (3–18%), cellulose (23–43%), and lignin (35–45%), [25], and a 6% of extractive [41]. For instance, Cristóvão and co-workers (2012) immobilized commercial laccase on coconut fiber by covalent attachment aided by sodium borohydride for decolorizing textile industry wastewater [9]. When the experiment was carried out at pH levels of 7.0 and 10.0, the immobilization efficiency was 74% and 50%, respectively. This biocatalyst decolored dyes with an efficiency of more than 80%, but the performance dropped to 20% after the third cycle, most likely due to the interaction of the dyes with the covalent attachment site of the fiber. In addition, de Souza Bezerra and colleagues (2015) used cross-linking process aided by glutaraldehyde to immobilize laccase on coconut fiber. Their finding indicated that yield was between 50% and 74%, which was used to clarify apple juice, and the system performed for 10 cycles [33]. Tomke and Rathod [37] produced a biocatalyst employing coconut biochar and peanut shell to immobilize lipase through covalent bonding aided by glutaraldehyde to synthesize cinnamyl acetate. The biocatalyst accomplished 94% of the transesterification process. Barbosa and co-workers (2020) used covalent bonding aided by glutaraldehyde and physical adsorption to immobilize peroxidase by employing coconut fibers as a carrier [4]. They stated that the system efficiency was 77.74% and 48.15%, covalent and physical adsorption, respectively. laccase derived from *Aspergillus flavu* was used by Ghosh and Ghosh [12] to be immobilized on coconut fiber. The findings revealed that the immobilized enzyme maintained 90% of its activity after four cycles and 50% after nine cycles. The lignin in coconut fibers serves as a substrate for laccase, enhancing its attachment to the carrier.

Considering the above-mentioned literature on enzyme immobilization on coconut fiber and to the best of the authors' knowledge, there has been no study on utilizing coconut shell biochar as a carrier for laccase immobilization. This research evaluates the synergistic and individual effects of adsorption and enzymatic degradation of laccase immobilized on three commercial coconut shell biochars for removing a range of pharmaceuticals such as diclofenac, amoxicillin, carbamazepine, and ciprofloxacin from water. The study also examined both systems' stability and long-term performance. These pharmaceuticals were selected due to their frequent occurrence in water bodies worldwide and their potential environmental and health risks [50]. Three of these pharmaceuticals, namely diclofenac, amoxicillin, and ciprofloxacin are on the updated watch list of the European Water Framework Directive [20]. Characterization of raw and loaded biochar is carried out to study the change in the surface chemistry of adsorbents and gain insights into the removal mechanisms. Adsorption and degradation kinetics and thermodynamics are also investigated to understand the nature of removal and its spontaneity.

2. Methodology and materials

2.1. Materials

Sigma-Aldrich supplied Nitric acid (HNO_3), and sulfuric acid (H_2SO_4). AVANTOR supplied the citric acid and Na_2HPO_4 necessary to make the McIlvaine citrate-phosphate solution. Merck KGaA provided the laccase enzyme (*Trametes versicolor* ($\geq$0.5 U mg^{-1}), fungal origin), diclofenac ($C_{14}H_{11}Cl_2NO_2$), amoxicillin ($C_{16}H_{19}N_3O_5S$), carbamazepine ($C_{15}H_{12}N_2O$), and ciprofloxacin ($C_{17}H_{18}FN_3O_3$). Roche Diagnostics GmbH supplied the 2,2′-azino-bis(3-ethylbenzothiazoline-6-sulfonic acid) diammonium salt (ABTS) (98%) for enzyme activity measurements. Other materials have been mentioned throughout the article were purchased from Sigma-Aldrich as well. Throughout the experiments, Ultra-pure water (abbreviated as MQ henceforth) from the Millipore Direct-Q® 5 UV purification system (resistivity$\geq$18.2 MΩ.cm) was utilized for cleaning and the preparation of the solutions. Whatman® glass microfiber filters were used to separate adsorbents from the aqueous media. Chemicals and reagents of analytical grade were used without further purification.

2.2. Granular activated carbons (GACs)

This research tested commercially available granular activated carbons (GACs) (Activated carbon 12 ×40 mesh, provided by AquaSorb® CT [2], Silcarbon K124 (IRIMEX) [16] GmbH, Germany and Donau, GmbH, Germany) prepared from coconut shells. GACs have a high surface area of 1100 m^2/g, 0.5 – 1.7 mm particle size, 500 kg/m^3 as bulk density, 4% ash content, and alkaline pH. Table S1 shows the essential characteristics of used GACs.

The adsorption capacity of activated carbon is influenced by its porous structure and surface area, but it is also greatly impacted by the surface functional groups. It is well-documented that activated carbons include the number of hydrogen atoms and heteroatoms, such as oxygen, nitrogen, chlorine, and sulfur [29]. The proportion of these atoms on the adsorbent's surface is often altered after the activation process. Oxygen groups (carboxyl groups, carbonyls, and lactones) are primarily a result of the oxidation of the raw material [36]. The number of nitrogenous groups depends on the nature of the raw material and is characteristic of carbons derived from coconut shells. By attracting positively charged ions such as metal ions, functional groups can facilitate bonding. Before chemical treatment, GACs were crushed and sieved through ~0.7–1 mm. GACs were rinsed with MQ water to remove fine particles and neutralize the pH. Then, they were left overnight at 60 °C to remove the moisture.

Approximately 4 g of each kind of GACs were placed into a 400 mL mixture comprising 5 M H_2SO_4 and 5 M HNO_3 (1:1) while being heated under reflux for 5 h at 80 °C. Samples were left to cool down, and the

GACs were rinsed multiple times to eliminate extra acid content and rinsed with MQ water till pH reached 6–7, following the protocol of Naghdi et al. [21]. The modified GACs (henceforth termed mAC (Activated carbon), mSIL (Silcarbon), and mDON (Donau)) were placed in an incubator (POL-EKO APARATURA, Poland) overnight to dry at 50°C. They were kept in separate, sealed bottles for later use.

2.3. Enzyme immobilization

This step followed our previous work [1,24]. In brief, a 50 mL Erlenmeyer flask contained 0.5 g of mGAC combined with 10 mL of pH 5 containing 2 mg mL^{-1} laccase. The combination was kept in a FAITHFUL® Instrument incubator at 30°C and 150 rpm for six hours. The samples were then deposited in 2 mL Eppendorf tubes and centrifuged at 10000 rpm for 2 min using FRONTIERTM 5515 R. To determine laccase immobilization, the starting activity was subtracted from the immobilized one. To eliminate unbound laccase prior to assessing the enzyme's activity, the mixture was rinsed two times with 2 mL of pH 5 (each). The final samples with immobilized laccase (denoted as LmGAC) were refrigerated to evaluate the optimal pH, temperature, stability, enzyme concentrations, and pollutant removal parameters.

2.4. Enzyme assay

By oxidizing ABTS (as a substrate), the free and immobilized laccase activities were measured and calculated [40]. At ambient temperature, the increase of absorbance at 420 nm (ϵ =36,000 M^{-1} cm^{-1}) was monitored. A UV–visible spectrophotometer type V-530 (Jasco) with a double beam was used for activity measurements. One unit of laccase activity corresponds to the amount of laccase required to oxidize one μmol of ABTS per minute under the conditions of the standard assay. A pH 5 buffer mixture containing 0.5 mM ABTS (375 μL), and 2 mg mL^{-1} of enzyme concentration (125 μL) was evaluated spectrophotometrically at room temperature. Throughout the mixing procedure, the color of the mixture shifted to blue due to the laccase oxidation of ABTS to ABTS radical. LmGAC activity was carried out by adding 20 mg in two milliliters of pH 5 comprising 0.5 mM ABTS with incubating for one minute. Eqs. (1) and (2) were used for activity measurements:

$$\text{Free laccase activity}\left(\text{U.mL}^{-1}\right) = \frac{\Delta abs \times D_f \times R_v}{\epsilon \times t \times E_v} \quad (1)$$

$$\text{Immobilized laccase activity}\left(\text{U.g}^{-1}\right) = \frac{\Delta abs \times D_f \times R_v}{\epsilon \times t \times M_{\text{carrier}}} \quad (2)$$

Where Δab is $ABTS^+$ absorbance, D_f is the factor of the dilution, R_v is the volume of the reaction (mL), ϵ is $ABTS^+$ an extinction coefficient, t is the time of the reaction (minute), $M_{carrier}$ is the carrier mass used for laccase immobilization (gram), and E_v is the enzyme volume (mL).

2.5. Enzyme optimization, reusability, and stability experiments

The laccase immobilization on mGAC was examined in different ranges of enzyme concentrations pH, and temperature. A pH range of 3–7, temperature of 10–50 °C, and laccase concentration range from 0.5 to 3 mg mL^{-1} were investigated. The immobilization yield (%) is calculated by dividing the difference between the enzyme activity in the supernatant before and after immobilization by the enzyme activity in the supernatant before immobilization [9]. The free and immobilized enzymes were evaluated for an hour across the pH range of 3–7 at 25 °C. The stabilities of free and immobilized enzymes were examined for an hour at temperatures range of 10–50 °C. The activity of free and immobilized laccase was examined every five days for a month. Using ABTS, the reusability of LmGAC was evaluated for up to six cycles.

The experiment on the reusability of LmGAC was performed to assess its cycle stability. About 25 mg of LmGAC was mixed with 5 mL of 0.5 mM ABTS at room temperature. The enzyme activity was then measured in the supernatant layer after the cocktail had been centrifuged at 10000 rpm for three minutes. After measuring each cycle, the LmGAC was rinsed two times to get rid of ABTS and re-equilibrated at pH 5 via a solution containing fresh ABTS. Accordingly, the cycle was repeated several times to evaluate the operational stability of the process.

2.6. GACs characterizations

2.6.1. SEM-EDX and S_{BET}

The morphology of unloaded and loaded adsorbents was investigated using SEM-EDS (FEI/Thermo-Fisher Apreo S LoVac SEM and AMETEK, USA). Micromeritics (3Flex) was used to evaluate the BET specific surface area and pore size distribution of AC, SIL, and DON within a liquid temperature of 77 K. Before the analysis, the samples were outgassed at 150 °C overnight to clean the surface. A relative pressure (P/P_0) of 0.95 was applied. Using the t-plot method, surface area and micropore volumes were calculated.

2.6.2. FTIR and titration

The FTIR spectrum can provide crucial information on the chemical structure and functional groups of a substance. FTIR (NicoletTM iSTM 5 FTIR, Thermo-Fisher, United States) coupled with an iD7 ATR accessory was used to acquire infrared spectra. The IR spectra were obtained with a resolution of 2 cm^{-1} with a range of 400–4000 cm^{-1}.

The Boehm titration was utilized to determine the amount of surface functional groups such as phenolic group (–OH), carboxylic group (–COOH), and carbonyl group (C═O) which are the most characteristic of activated carbons [6]. About 0.5 g of each mGACs (mAC, mSIL, and mDON) was combined with 50 mL of solutions of 0.05 N HCl, NaOH, $NaHCO_3$, Na_2CO_3, and C_2H_5ONa, respectively. After 24 h of constant agitation at 150 rpm and 25 °C, the carbon-containing suspensions were membrane filtered. Then, depending on the starting solution, 10 mL aliquots of acid or base filtrate were titrated with 0.05 N NaOH or HCl. For each reaction, blank samples were performed under similar operating conditions. The resulting solutions were pH adjusted till neutrality. The following determinations were used for the number of acidic groups on the mGACs (mAC, mSIL, and mDON): Na_2CO_3 neutralized lactones and carboxylic. Moreover, $NaHCO_3$ neutralized only carboxyl groups. Furthermore, C_2H_5ONa neutralized carboxylic, carbonyl, lactone, and phenolic groups. On the other hand, total acidic functional groups neutralized by NaOH. The quantity of basic surface sites is determined by the quantity of HCl that interacts with activated carbon. The differential in acid/base strength governs the response between functional groups (acidic oxygenated) and reagents on the surface.

2.7. HPLC measurements

Diclofenac (DCF), Amoxicillin (AMO), Carbamazepine (CBZ), and Ciprofloxacin (CIPRO) were utilized as emerging pollutants' models. Using high-performance liquid chromatography, pharmaceutical degradations were determined. The measurements were accomplished by Merck-Hitachi D-7000 HPLC instrument. HPLC column was Zorbax SB-Aq with a dimension of 150 mm length × 4.6 mm Diameter, 5 μm particle size (Agilent, Santa Clara, CA, USA) with gradient elution. The injected sample volume was 10 μL. The mobile phase consisted of 0.1 V/V% trifuoroacetic acid in MQ water as eluent A and methanol as eluent B. The gradient program consists of 0 −1 min 40% mobile phase B and 1–5 min gradient up to 100% mobile phase B. This was continued for up to 8 min. After this, the gradient was returned to the initial stage. The flow rate was adjusted to 1 mL min^{-1}. Under this condition, the calibrations of the compounds were linear between 5 and 100 μg mL^{-1}. The retention time of DCF, AMO, CBZ and CIPRO was detected at 7.15, 2.46, 6.34, and 4.54 min, respectively. The standard deviations (SD) were 0.011, 0.008, 0.011 and 0.009 min for DCF, AMO, CBZ and CIPRO,

respectively.

The degradation of DCF, AMO, CBZ, and CIPRO was accomplished by adding 250 mg of LmGAC to 0.075 L of a matrix comprising 50 mg L^{-1} of the chemicals with continuous shaking at 150 rpm. After 120 min, 2 mL of the samples' supernatant was taken every 30 min. Due to the selectivity of the enzyme catalytic process, the adsorption of chemicals is possible [48]. In order to analyze the adsorption of pharmaceutical compounds without immobilization, further sets of experiments have been conducted. The adsorption of the chemicals in these experiments was measured for 120 min at 30 °C. Every 30 min, 2 mL of the supernatant was gathered and analyzed using HPLC.

2.8. LmGACs and mGACs reusability

The reusability of both LmGAC and mGAC was examined by removing DCF, AMO, CBZ, and CIPRO. In batches, degradation and adsorption studies were conducted on pharmaceutical compounds (Section 2.7). After 120 min (duration of each cycle), the samples were washed via pH, centrifuged, and the recovered carbons were reutilized. On a few occasions, however, carbons were not completely recovered by washing. To preserve the solids-to-liquids ratio as the first batch, the LmGAC and mGAC amount was adjusted after each cycle.

2.9. Enzyme kinetic, adsorption isotherms, kinetics, and thermodynamics

This section is explained in detail in Text S1 in the supplementary materials.

2.10. Data visualization and check

Results are presented in mean and standard deviation, and experiments performed in triplicate. The software Origin Lab 2019 was used for analyzing the data that had been checked using the Kolmogorov-Smirnov test at the 0.05 level of significance.

3. Results and discussions

3.1. mGACs characterization

Fig. 1 shows the SEM and EDX for GACs and mGACs. In terms of the surface morphology of the GACs, the micrograph of untreated GACs reveals a homogenous surface with pores dispersed throughout its surface. The surface of mGACs treated with mineral acids showed a more heterogeneous surface with deeper pores, which could be attributed to the acid treatment's actions that typically remove impurities from carbon pores [24]. In a similar investigation, Lonappan and co-workers (2020) reported that biochar treated with citric acid formed more

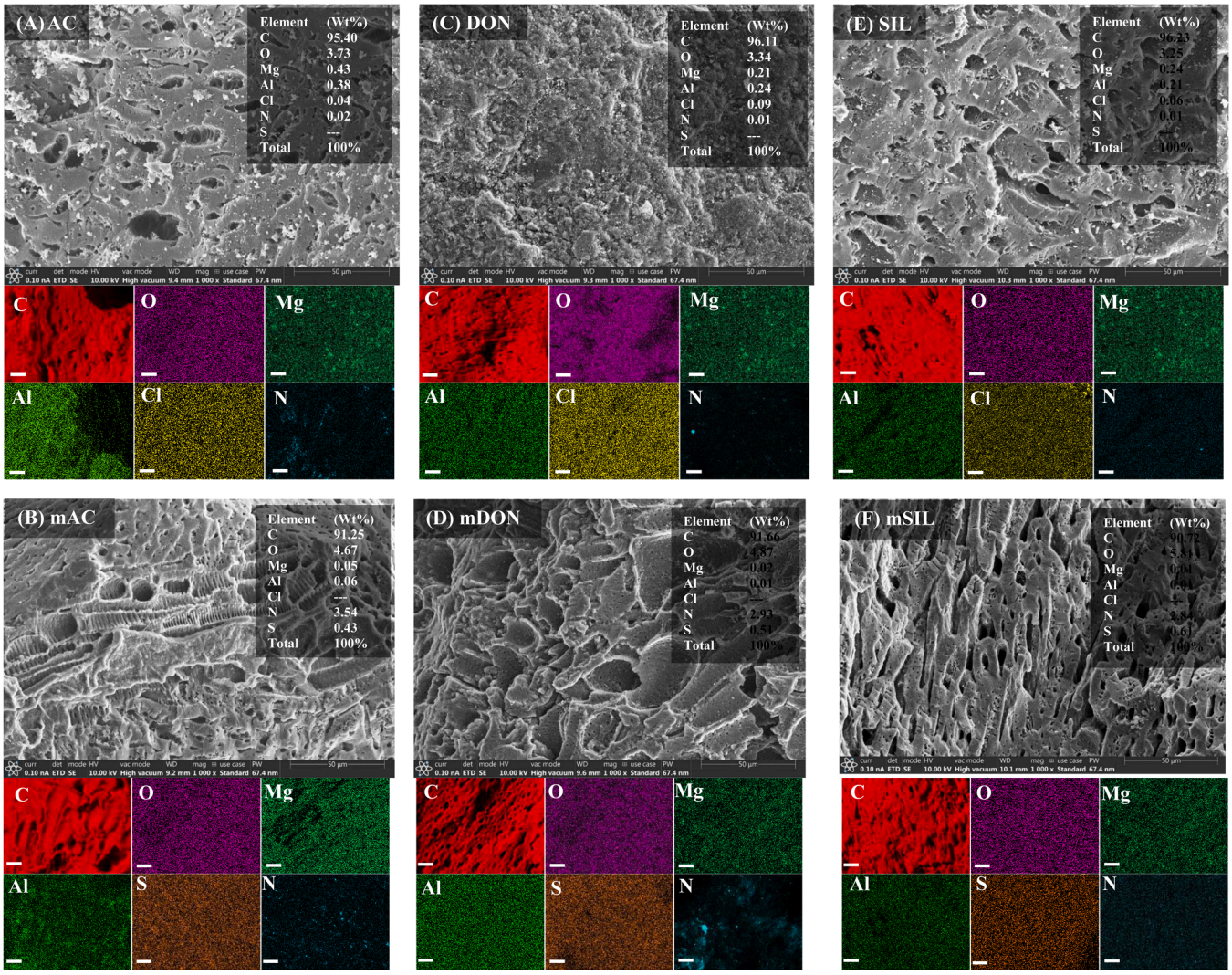

Fig. 1. SEM and EDX before and after the modification for AC (A), mAC (B), DON (C), mDON (D), SIL (E), and mSIL (F). (Other SEM pictures for LmGACs and LmGACs after removal are illustrated in Fig. S1). EDX scale is 5 μm.

porous structures [18]. Fig. S1 illustrates the SEM for LmAC, LmDON, LmSIL, and LmGACs after removal. Scanning micrographs of the immobilized enzyme did not reveal any significant surface topography alterations. This is probably owing to the small size of the laccase protein (60–90 kDa) [24], which corresponds to a particle size of less than 5 nm. This dimension is difficult to capture by micrographs with a 1 μm magnification [19]. However, following enzyme immobilization, the surface of LmGACs seemed smoother, probably due to enzyme coating on the biochar surface [51], as illustrated in Fig. S1. Enzyme immobilization in magnetic biochar nanoparticles has been linked to a smoothing of the surface and a coating-like shape [13].

The structure of the surface of functionalized mGACs is homogeneous and porous. The inclusion of mesoporous, microporous, and macroporous on mGACs enhances the heterogeneous surface accessibility for adsorption. The EDS analysis revealed the distribution of elements in the original and modified adsorbents, which is essential for comprehending the chemical reaction occurring throughout the modification process. Fig. 1 shows that GACs had elements of C, O, Mg, Al, Cl, and N at the surface. All samples contained oxygen, indicating the presence of oxygen-containing groups on the surface. Elements of N and S, emerged in mAC, mSIL, and mDON compared with untreated GAC. Cl in the original GAC disappeared after treatment with mineral acids, while Mg and Al concentrations decreased indicating that chemical reactions occurred during the treatment.

Table S2 displays the findings of surface functional groups for different samples of treated and untreated GACs. The overall oxygen-containing functional group content of the original GAC was 0.32, 0.4, and 0.36 mmol g^{-1} for AC, SIL, and DON respectively. Phenolic and lactone groups were 68.7%, 31.3% for AC, 62.5%, 37.5% SIL and 63.9%, 36.1% for DON. Furthermore, no carboxylic group was found in the AC, SIL, and DON. The total basic were 0.12, 0.21, and 0.16 mmol g^{-1} for AC, SIL, and DON respectively. The overall concentration of oxygen-containing functional groups increased considerably from 0.32 to 3.5, 0.4–3, and 0.36–3.16 mmol g^{-1} for mAC, mSIL and mDON, respectively. The carboxylic group increased significantly from zero in all GACs to 2.2, 1.9, and 1.66 mmol g^{-1} for mAC, mSIL and mDON respectively, contributing to the high oxidation ability of treated adsorbents.

The FTIR spectra of the examined adsorbents were recorded in order to have a better understanding of the functional groups present on the surface. As demonstrated in Fig. S2, all samples had CH_2 stretching bands at 2920 and 2844 cm^{-1}, which were asymmetrical and symmetrical, respectively. Carbonyl group (1630 cm^{-1}) and phenolic group (1118 cm^{-1}) absorption bands were found in the original GAC, mAC, mSIL, and mDON. In addition, mAC, mSIL, and mDON exhibited C═O stretching at 1384 cm^{-1} due to chemical treatment by H_2SO_4 and HNO_3. The peaks between 1380 and 1390 cm^{-1} displayed the –COOH absorption band. In general, the FTIR analysis agrees with Boehm titration results. The addition of laccase had a very subtle effect on the FTIR spectra of modified adsorbents represented by the slight increase in the intensities and broadening of the peaks at 3400 cm^{-1}, 1600 cm^{-1} and 1160 cm^{-1}. The peak at 3400 is associated with the overlapping of O-H and N-H bond of laccase [31]. Peak in 1600 cm^{-1} is believed to be linked to N-H stretching vibration which is regarded as an indication of laccase protein presence [14]. Peaks in the range of 948–1165 cm^{-1} have been reported to be characteristics of laccase protein [31].

The BET surface area of the raw GACs as based on the datasheet was 1100 m^2 g^{-1}. The tested sample surface areas were marginally lower than the quoted figures by the supplying companies with 1050, 1010, and 1003 m^2 g^{-1} for AC, DON, and SIL, respectively. Table S3 shows the BET surface areas for GACs and mGACs. It was found that 1.173, 0.342, and 0.831 cm^3 g^{-1} were the total pore, micropore, and mesopore volumes of AC, respectively. However, they were 0.913, 0.322, and 0.591 cm^3 g^{-1} for DON and 0.858, 0.357, and 0.501 cm^3 g^{-1} for SIL. After the modification process, a further 18–19% increase was noticed in the adsorbents' surface areas.

3.2. Enzyme immobilization

Laccase immobilization on LmGACs was achieved using the adsorption approach. To enhance laccase immobilization, pH and temperature ranges were used to optimize immobilization conditions. The pH of the matrix influences the stability of the enzyme; thus, it is an essential component to consider throughout the immobilization process. The impact of altering pH (A), temperatures (B), laccase concentrations (C), and immobilization yield (D) is shown in Fig. 2. Consistently, the impact was assessed by measuring ABTS activity. Fig. 2 (A) demonstrates that at pH 3, laccase immobilization is low, perhaps due to a loss of laccase activity, but increases progressively at pH 4, and reaches its maximum at pH 5 with 35, 29.7, and 28.8 U g^{-1} for LmAC, LmSil, and LmDon respectively. At pH6, the laccase immobilization decreased by 10.2, 6.4, and 7.9 U g^{-1} for LmAC, LmSil, and LmDon respectively. Afterward, the laccase immobilization dropped significantly at pH7 to reach 16.2, 15.4 and 14.1 U g^{-1} for LmAC, LmSil and LmDon respectively. Temperature is another critical factor of laccase immobilization since the enzyme is temperature-sensitive and only functions within its optimal heat range. Enzyme immobilization enhanced from 35.3 to 53.9 U g^{-1}, 31.7–51.3 U g^{-1} and 30.5–47.5 U g^{-1} for LmAC, LmSil, and LmDon respectively once the temperature increased from 10° to 30°C as depicted in Fig. 2 (B). This is because of the accelerated rate of enzyme adsorption on LmGACs. At 50 °C, the rate of enzyme immobilization reduced to 11.4, 8.8, and 6.2 U g^{-1} for LmAC, LmSil, and LmDon respectively, possibly due to a decrease in enzyme viability as the temperature is raised [45].

Rising the enzyme concentrations from 0.5 to 2 mg mL^{-1} increased the immobilization from 13.5 to 61.8, 18.2–57.5, and 15.3–54.1 U g^{-1} for LmAC, LmSIL, and LmDON, respectively, as shown in Fig. 2 (C). Nevertheless, raising the enzyme concentration over 2 mg mL^{-1} had no impact on laccase immobilization owing to the diminishing of accessible sites on the surface of mGACs. The laccase immobilization yield was tested for optimum temperature and concentration with various pH environments as depicted in Fig. 2 (D). The highest immobilization yield was obtained at pH = 5 at 65.2%, 63.1%, and 62.9% for LmAC, LmSIL, and LmDON, respectively. The high immobilization yield obtained from this system within the optimal conditions could be owing to the presence of carbonyl groups [19]. Other investigations have shown a little higher immobilization yield. Imam and colleagues (2021) examined the utilization of laccase immobilized on the surface of acid-treated rice husk biochar for anthracene biodegradation [15]. The findings showed that acid-treated biochar immobilized laccase had a high immobilization yield of 66% and high operational stability. In addition, this immobilized system completely degraded 50 mg L^{-1} anthracene in aqueous batch mode within 24 h. Garca-Delgado and co-worker [10] studied biochar (holm oak (*Quercus ilex*)) immobilized laccases, which were evaluated to remove three tetracyclines and six sulfonamides at a concentration of 0.1 mmol L^{-1} of each antibiotic. High levels of activity yields (70.3%) and catalytic capacities (1405 IU g^{-1}) were achieved using *Pleurotus eryngii* laccase on biochar. In the presence of syringaldehyde, only chlortetracycline was completely eliminated, while immobilized-laccase/ABTS systems cleared all tetracyclines. This demonstrates that a slight alteration of LmGACs rendered it a suitable host for laccase.

3.3. LmGACs stabilities and reusability

Fig. 3 demonstrates the stability of the immobilized and free enzyme in relation to pH (A), and temperature (B). LmGACs are more stable than free laccase in most tested pH and temperatures, likely due to their decreased structural pliability and enhanced rigidity, which promotes their stabilities under varying pH conditions [8]. At pH 5, LmGAC stabilities demonstrated an 8% improvement in activity over that of free enzyme. In pHs, the stabilities of LmGACs were greater than that of free laccase, with optimal activities reported for LmGACs at pH 5, except at

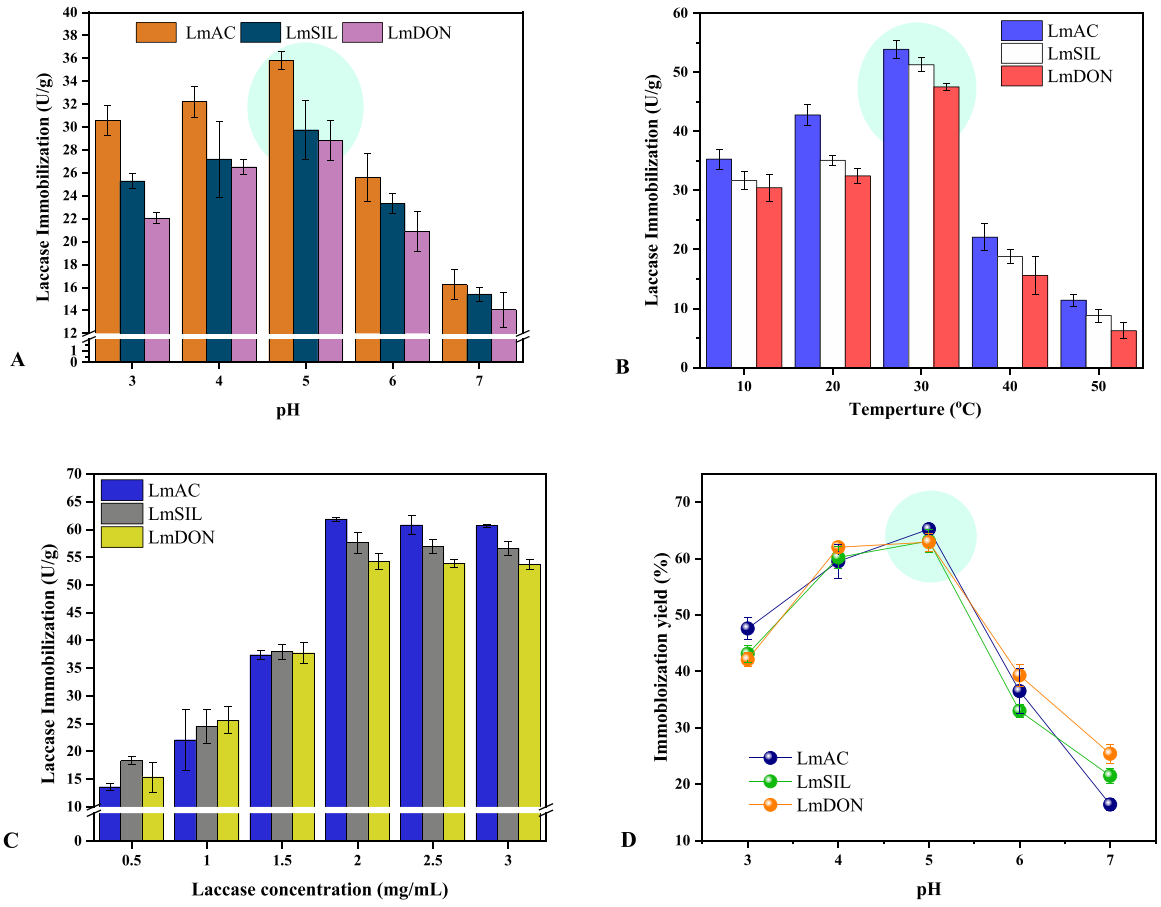

Fig. 2. The impact of changing pH (A), temperatures (B), laccase concentrations (C) on immobilization and yield (D).

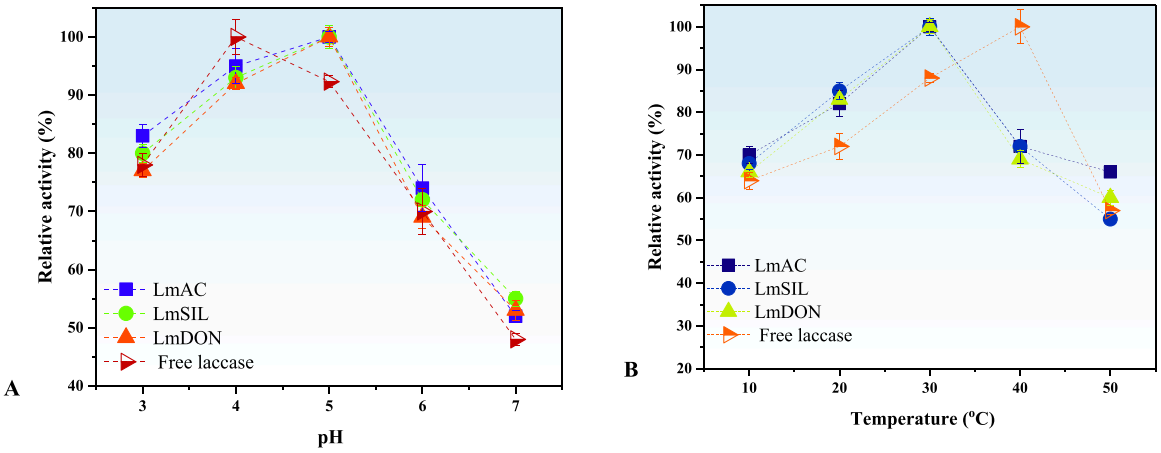

Fig. 3. Free and immobilized enzyme stability on mGACs related to pH (A), and temperature (B).

pH 4, when the free enzyme demonstrated activity superior to the immobilized enzyme. The loss of laccase activity at high pH is likely attributed to enzyme denaturation. The wider active pH range of immobilized laccase is probably due to the presence of functional groups on the adsorbent's surface that can scavenge H^+ from the solution and maintain the enzyme activities [31]. In temperature measurements, free and immobilized laccase displayed a respective optimal temperature of ~40 °C and ~30 °C. Afterward, it showed a drop with increasing temperature. This variation was more apparent for the free enzyme than for the immobilized one. Similar trends were observed in the literature with a bit of variation in the optimal temperature. The optimal temperature of free and immobilized laccase (from *Aspergillus*) on silica nanoparticles was 40 °C and 50 °C, respectively [14]. Another study showed that both free and immobilized laccase (from *Trametes versicolor*) on metal-organic framework had the highest activities at 30 °C [31]. The variation in the optimal activity temperature of free and immobilized laccase is due to the difference in laccase orgin and the support materials.

As demonstrated in Fig. 4, the stability of free and immobilized enzymes was assessed by keeping them at 4 °C and 25 °C and evaluating their activity every five days for up to one month. The LmGACs are better than the free enzyme because of their higher storage stability, which is a key factor in determining an enzyme's efficiency.

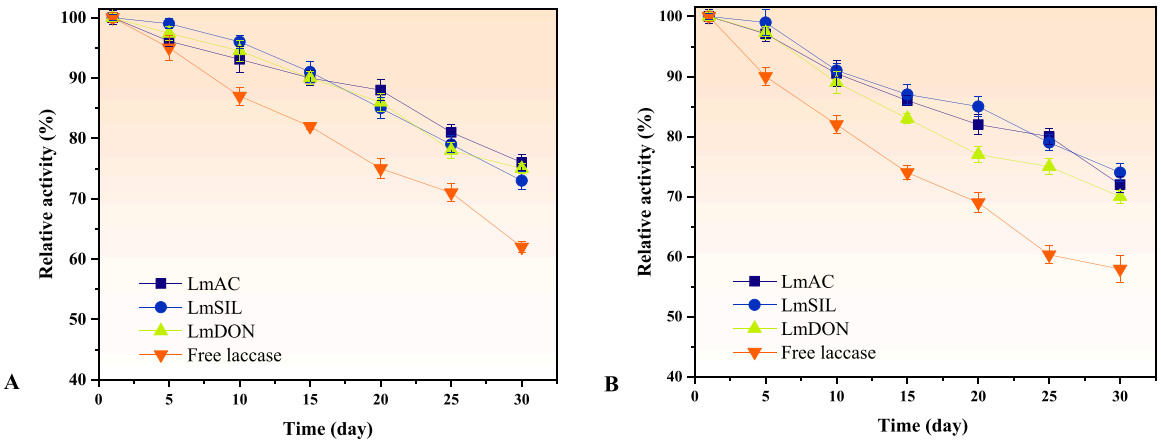

Fig. 4. Stability of free and immobilized laccase on mGACs related storage duration with 4 °C (A) and 25 °C (B).

Immobilization reduces oxidative and reduction losses, the two primary causes of activity decline in storage. Compared to free laccase, bound laccase was more stable during storage because of its reduced conformational changes [30]. After four weeks, the relative activity of the immobilized enzyme at 25 °C decreased to 72%, 74%, and 70% for LmAC, LmSIL, and LmDon respectively, while free laccase showed a 42% drop in relative activity. The relative activity at 4 °C storage displayed a better performance in both cases. The relative activity of immobilized laccase reduced to 76%, 73%, and 75% for LmAC, LmSIL, and LmDon, respectively, whereas it was about a 38% drop in the case of free laccase. The difference between the support materials is marginal suggesting that they can equally be used for immobilization. As low temperatures aid in preserving the proper conformation and orientation of the enzyme, it was anticipated that the immobilized enzyme would be more stable when refrigerated than when kept at room temperature. The observations of this work agree with those of earlier studies, such as Zhang et al. [51] who examined the stability of immobilized enzyme by adsorption and cross-linking in biochar. Laccase retained 81.8% and 64.4% of its initial activity after one month of storage at 4 °C and 25 °C, respectively. In another work, Naghdi and co-workers (2019) immobilized laccase by encapsulating it in biochar; after around 1.17 months of storage at two different temperatures, laccase activity remained at 31% and 17%, for 4 °C and 25 °C, respectively [22].

The stability of immobilized laccase is an essential evaluation factor. During the course of the batch experiment investigation, the operational stability of the LmGACs systems was evaluated across a number of successive cycles. Fig. S3 depicts the results of measuring the LmGACs' activity during this procedure. No activity loss was observed in the first cycle, whereas reductions of 3%, 7%, and 18% were recorded during the 2nd, 3rd, and 4th cycles, respectively. In the last two cycles, the activity of immobilized laccase decreased significantly, especially for LmSIL and LmDON. During the 2nd, 3rd, and 4th cycles, revealed LmSIL activity drops of 5%, 9%, and 14%, respectively. The LmSIL activity decreased by 43% and 66% during the fifth and sixth cycles, respectively. LmDON activity had reductions of 7%, 12%, and 23% over the 2nd, 3rd, and 4th cycles, respectively. In the last two cycles, the LmDON activity decreased by 41% and 69%, respectively. LmAC exhibited more or less similar reduction trends as those of LmSIL and LmDON for all cycles except for the last cycle where it had almost double the activities of the other composites.

The reduction in enzyme activity could be attributed to laccase leakage from the support and laccase denaturation. The observed decrease in activity is to a certain extent similar to previous research results [1,15,45]. For instance, Wang and coworkers immobilized laccase by adsorbing it onto biochar layered with cetyltrimethylammonium bromide. Following 6 cycles, the isolated enzyme had decreased by nearly 55% of its activity. Six rounds of enzyme immobilization on rice straw biochar retained approximately 40% of its starting activity, according to a study by Imam and researchers (2021) [15]. Zhang and collaborators (2014) detected a 70% drop-in immobilized enzyme activity on a nanofiber membrane after 10 dye-removal ABTS-oxidation cycles [49]. In the present investigation, the immobilized enzyme revealed satisfactory stability and reusability. High interactions between mGACs and enzyme, which allow for its effective immobilization, are principally responsible for the high operational stability of the immobilized enzyme.

Both free and immobilized laccase exhibited a typical behavior of an enzyme reaction with the substrate ABTS. Accordingly, the Michaelis–Menten equation was used to estimate the kinetic parameters. K_m and v_{max} were found by nonlinearly fitting reaction rate versus substrate concentration. Fig. S4 shows LmGACs and free enzyme Michaelis–Menten fitting model. It is well known that the value K_m indicates the enzyme's affinity for the substrate. The K_m value decreased from 0.516 mM (free laccase) to 0.413, 0.396, and 0.405 mM for LmAC, LmSIL, and LmDON respectively. It can be deduced that immobilization decreases the affinity of laccase for ABTS. This might be due to mass transfer constraints between the ABTS and the surface of adsorbents. The minute changes in the three-dimensional conformation of the enzyme during adsorption onto the carrier have direct or indirect effects on the laccase's active site [9]. Other investigations have obtained similar results demonstrating a lower affinity for the substrate because of the diffusional restrictions and decreased enzyme flexibility following immobilization [43,7]. The immobilized enzyme has a lower v_{max} value of 5.904, 5.507, and 4.967 mM min^{-1} for LmAC, LmSIL, and LmDON respectively compared to the free enzyme (9.24 mM min^{-1}). The establishment of substrate diffusional constraints following enzyme binding may account for the decreased maximal reaction rate.

3.4. Isotherms, kinetics, and thermodynamics

The results of fitting experimental data to Langmuir and Freundlich isotherm models are shown in Fig. 5. Langmuir isotherm model fits the pharmaceutical compounds adsorption data better with high correlation coefficients ranging from 0.903 (for CBZ on mAC) to 0.995 (for DCF on mAC) compared to the Freundlich model with correlation coefficients between 0.775 (for DCF on mDON) to 0.988 (for AMO on mAC). This suggests the formation of a monolayer of pharmaceutical molecules on the surface of the adsorbent. The sorption capacity (q_m) was determined to be in the range of 180.5–735.2 mg g^{-1} for CBZ and AMO on mDON, respectively.

The R_L values for pharmaceutical compounds are between 0 and 1 as shown in Table S4, demonstrating favorable adsorption. According to Ghaedi and colleagues (2013), the value of n is less than one which also indicates that adsorption is favorable [11]. The value of 1/n, which

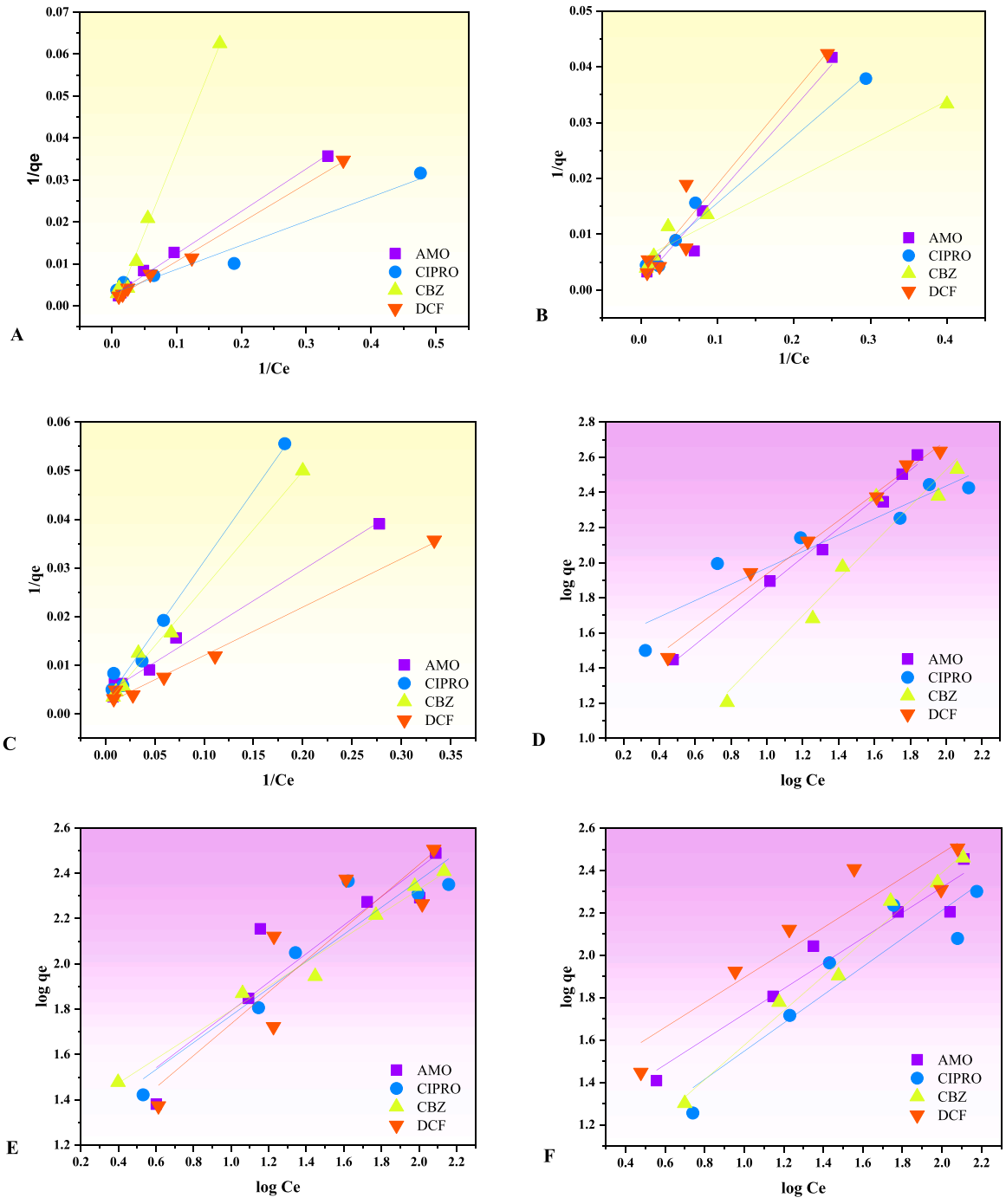

Fig. 5. Langmuir and Freundlich isotherm models fittings for mAC (A, D), mDON (B, E), and mSIL(C, F).

ranges from zero to one is referred to as the heterogeneity factor. In this investigation, the 1/n values for pharmaceutical compounds ranged from ~0.5 to ~1 suggesting a decreased degree of surface heterogeneity.

Fig. 6 illustrates the pseudo-first-order model and pseudo-second-order model for pharmaceutical compound adsorption. The correlation coefficients for the experimental data were fitted to the pseudo-first-order kinetic model which was between 0.933 (CIPRO adsorption with mAC) to 0.992 (AMO adsorption with mAC). This shows that physisorption limits the adsorption rate of the particles onto the adsorbent. Table S4 lists the fitting parameters for kinetic models.

The assessment of the thermodynamic parameters of pharmaceutical compounds on modified adsorbents is shown in Fig. S5. Table S5 displays the thermodynamic parameters of pharmaceutical compounds adsorption, including free energy (G°), enthalpy change (H°), and entropy change (S°), at different temperatures (i.e., 283, 293, 303, and 313 K). G° values decreased as the temperature rise, suggesting that temperature has a beneficial influence on the efficacy of adsorption. Negative values of G° measured at four different temperatures indicate that pharmaceutical compounds spontaneously adsorb onto mGACs. As positive H° values were recorded, it was determined that the adsorption process was endothermic. Positive S° values indicate that the adsorption process is steady as well as random [46].

3.5. DCF, AMO, CBZ, and CIPRO removal and reusability

Using LmGACs, this research evaluated the biodegradation of DCF,

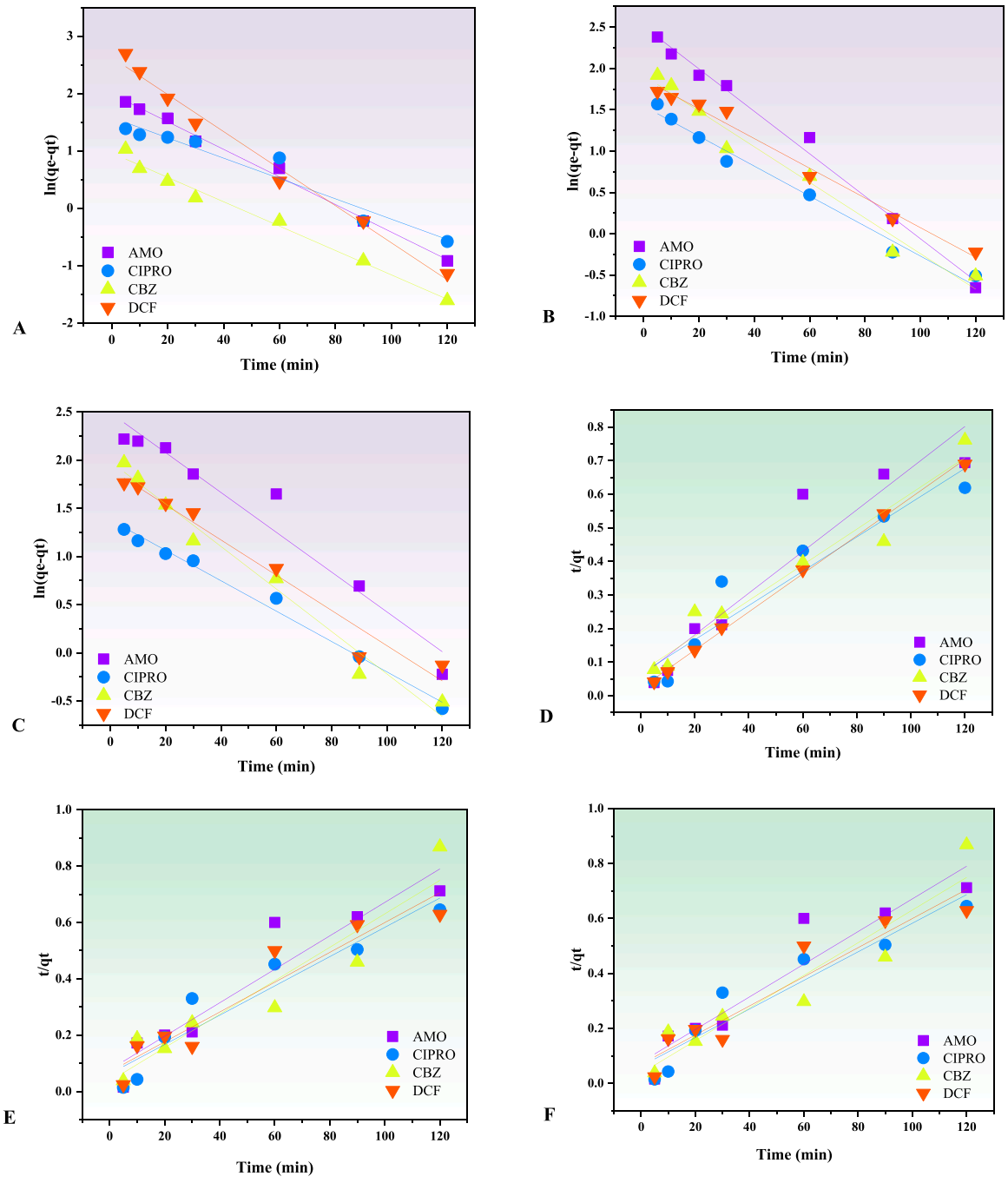

Fig. 6. Adsorption kinetics of pharmaceuticals using mAC (A, D), mDON (B, E), and mSIL (C, F).

AMO, CBZ, and CIPRO. The adsorption of DCF, AMO, CBZ, and CIPRO onto mGACs was also evaluated using controlled experiments. Fig. 7 represents the drop in DCF, AMO, CBZ, and CIPRO concentrations examined with the mGAC and LmGAC over a period of 120 min. The letter A denotes the removal with adsorption only, and the letter L refers to the combined removal through adsorption and enzymatic degradation. In the case of LmGAC, the reduction in DCF, AMO, CBZ and CIPRO concentrations was ascribed to the synergistic impacts of the laccase degradation as well as adsorption. DCF, AMO, CBZ, and CIPRO values were assessed by their corresponding retention times (7.14, 2.45, 6.34, and 4.52 min) and the area under the curve. The highest compound removed through adsorption was CIPRO for all adsorbents used, followed by DCF, CBZ, and AMO. The pharmaceuticals removal percentage through adsorption varies from the 20 s level to the 70 s level for the treatment time range of 30–120 mins. Incorporating laccase into the adsorbents increased the removal from 50% to almost 100% for all pharmaceuticals and adsorbents when treatment time increased from 30 min to 120 min. CIPRO continued to be the highest-removed pharmaceutical even after the introduction of laccase.

Because of the availability of adsorption sites as well as biodegradation on LmGACs, two assumed pharmacological removal processes occur. It is anticipated that adsorption onto free sites of LmGACs takes place first, and then adsorbed pharmaceuticals are degraded by laccases freeing more adsorption sites for attracting fresh pharmaceuticals from the bulk solution. This system proves its feasibility as an effective removal technique, however, the capacity of the system to regenerate and restore its properties is important, and this is what was investigated for 6 cycles, as shown in Fig. 8. In general, AC had the best removal

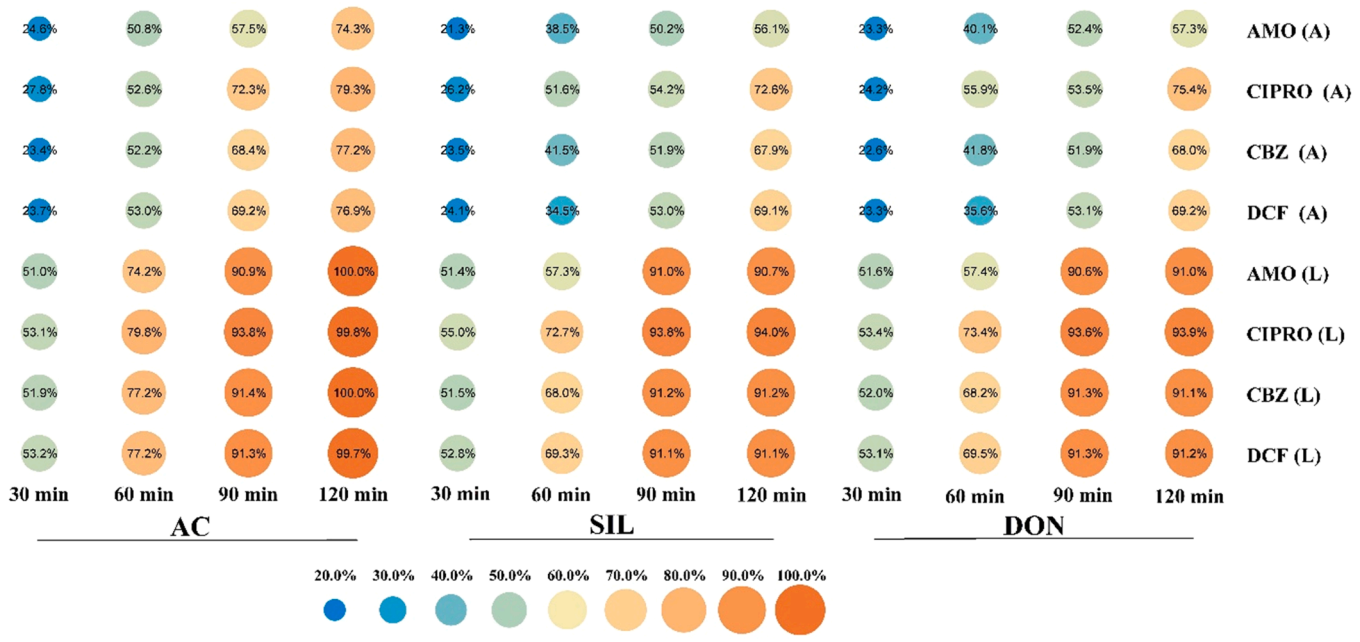

Fig. 7. AMO, CIPRO, CBZ, and DCF removal (%) with modified adsorbents and immobilized laccase on modified adsorbents.

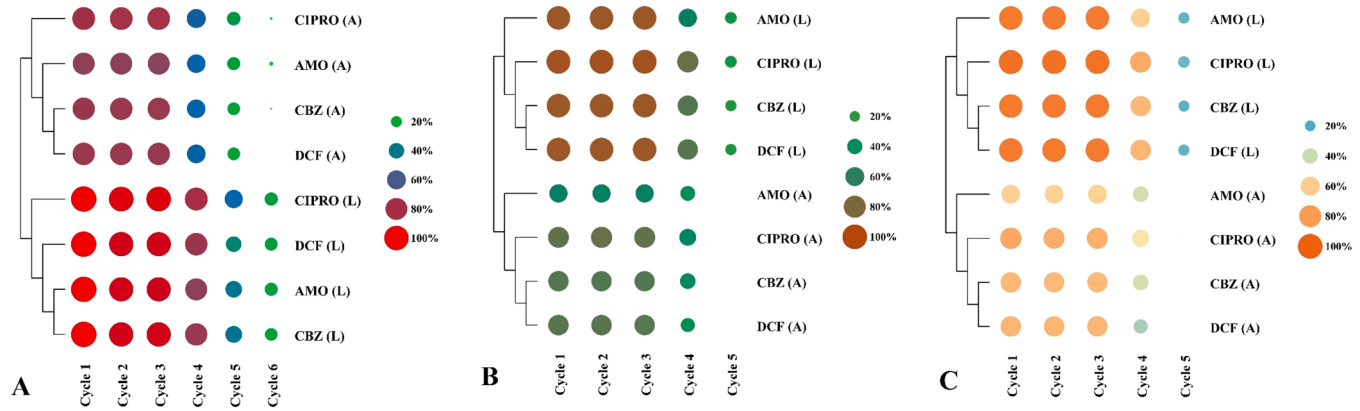

Fig. 8. The removal efficiency of AMO, CIPRO, CBZ, and DCF on AC (A), SIL (B) and DON (C) over 6 sequential cycles using the LmGACs and mGACs. The standard deviations were $\leq$ 3.29% for mGACs and $\leq$ 1.98% for LmGACs for all cycles.

performance, followed by DON and then SIL. As the number of cycles increased, the removal drops in all adsorbents and for all pharmaceuticals. The removal by the effect of adsorption diminishes after cycle 5. However, the addition of laccase prolonged the working life of the system. Even after 5 cycles, there is more than 20% can still be achieved for all adsorbents with tested pharmaceuticals. The decrease in the removal for both adsorption and combined adsorption with enzymatic degradation is small ($\leq$ 10%). The decreasing trend in removal efficiency (Fig. 8) could be attributed to the leaching and denaturation of the laccase, as was observed for ABTS oxidation [34]. Table S6 shows selected literature for pollutant removal by different conventional and new methods.

This system can potentially be used as a polishing method for wastewater effluent. Nonetheless, it is essential to explore the costs of the approach and optimize the operational factors for a broader range of emerging contaminants. Fig. S6 depicts the conceptual mechanism through which LmGACs absorb and degrade AMO, CIPRO, CBZ, and DCF. In general, common adsorption mechanisms such as hydrogen and π-π interactions (physical adsorption) and covalent bonding (chemical contact) are likely to be involved in removing pharmaceuticals from the solution. The adsorbed pharmaceuticals then get degraded by enzymes hosted by the porous structure of adsorbents. Functional groups play a crucial role in the interaction between enzyme and mGACs surface. Enzymes can transform aromatic functional groups on AMO, CIPRO, CBZ, and DCF into free radicals that trigger domino reactions [3].

4. Economical and environmental benefits

The cost of the immobilization support matrix accounts for about 47% of the total price of an immobilized enzyme system [38,5]. As such, carbon-rich precursor materials as investigated in this work can be used to alleviate the system cost and create matrices for enzyme immobilization. These precursors include agricultural, industrial, and domestic wastes which are easily obtainable and cost-effective. Moreover, its use in the immobilization matrices as a solid carrier will improve waste management while being economically viable, consequently encouraging sustainability on several levels. Furthermore, the immobilized laccase maintained a high removal rate of emerging pollutant mixtures within 5–6 successive reuses. This demonstrated that it would be more suited for the water treatment technique than laccase in its free form.

Recycling immobilized enzyme in a technological process has significant cost-cutting advantages.

5. Challenges and the way forward

Among the challenges of the enzyme immobilization approach is the identification of appropriate feedstock for matrix formation and the selection of suitable matrices for immobilizing the enzymes for varied purposes. This should also be accompanied by proper modification and functionalization to achieve maximum efficiency. Moreover, considerable barriers remain in the way of their larger-scale application, necessitating extra rigorous investigation to remove these constraints. Difficulty abounds in identifying the optimal immobilization approach from among the plethora of methods available and the preferred operating needs pertaining to agricultural waste characteristics. In addition, there is no molecular structure model for matrices such as biochar, despite the fact that much research has been undertaken on their efficacy in enzyme immobilization. It is crucial to construct a molecular structural model for biochar since it could assist give additional information about biochar's reactivity. This also could facilitate the functionalization of the material for various applications. Moreover, the utilization of purified enzymes instead of crude extract boosts the price of biocatalysis, which could also be thoroughly researched. In addition to the use of agricultural waste as support materials, an immobilized system should maintain activity through numerous subsequent cycles in order to reduce the cost per usage.

6. Conclusion

This study evaluated the removal of emerging pollutants (diclofenac, amoxicillin, carbamazepine, and ciprofloxacin) using three types of GACs immobilized with laccase (Activated carbon, Silcarbon, and Donau). A temperature of 30 °C, pH 5, and a laccase concentration of 2 mg mL^{-1} were shown to be the optimal immobilization factors for getting functional enzyme on the surfaces of the three adsorbents. The yields of laccase immobilization were 65.2%, 63.1%, and 62.9% for activated carbon, Silcarbon, and Donau, respectively, using the optimal settings. Emerging pollutant adsorption onto the tested activated carbon can be described as a spontaneous first-order reaction with endothermic nature following Langmuir isotherm. A rapid complete removal (within 120 min) of the pharmaceutical compounds (50 mg L^{-1}) was achieved with activated carbon, while more than 90% removal was achieved with other GACs through the immobilization process. However, ~70% of pollutant removal was achieved through the adsorption route only with activated carbon and 50–60% with other adsorbents. Stability performance tests for 6 cycles showed that the removal with adsorption only completely diminished after the fifth cycle, whereas, with laccase integration, it was possible to obtain a further 20–30% in the sixth cycle. The immobilized adsorbents with laccase can effectively be used for pharmaceuticals removal for up to three cycles where the removal varies between 90% and 100%. After 3 cycles, the regeneration might not be economically sound to be performed as the removal drops significantly. This study showed that the commercially available activated carbon originating from coconut shells can be used as supporting materials for constructing adsorption-enzymatic systems for emerging pollutant removal with reasonable stability and reusability. The potential application for this system is as a polishing treatment for wastewater treatment effluent. However, further studies into the technique's robustness with a more complex sample matrix are required. Aspects such as the competitiveness between pharmaceuticals and other contaminants for adsorption sites and their interaction with enzymes are of special interest. System design parameters for a continuous large-scale process should be explored too.

Fund

The ÚNKP-22–3-I-PE-12 (Osamah J. Al-sareji) New National Excellence Program of the Ministry for Culture and Innovation from the source of the National Research, Development and Innovation Fund supported this research.

CRediT authorship contribution statement

Osamah J. Al-sareji: Formal analysis, Data curation, Visualization, Methodology, Investigation, Resources, Conceptualization, Funding acquisition, Software, Validation, Writing - original draft, Writing - review & editing. **Mónika Meiczinger:** Supervision, Methodology, Validation, Resources, Writing - review & editing. **Viola Somogyi:** Supervision, Validation, Resources, Writing - review & editing. **Raed A. Al-Juboori:** Writing – review & editing, Methodology, Investigation. **Ruqayah Ali Grmasha:** Writing – review & editing, Methodology, Visualization. **Csilla Stenger-Kovács:** Methodology. **Khalid S. Hashim:** Methodology, Data curation, Writing - review & editing.

Declaration of Competing Interest

The authors declare that they have no known competing financial interests or personal relationships that could have appeared to influence the work reported in this paper.

Data Availability

No data was used for the research described in the article.

Acknowledgments

The authors are appreciative of the warm work of the editor and the anonymous reviewers earnestly. The authors thank the support provided by Liverpool John Moors University, United Kingdom, as well as Aalto University, Finland in different facilities. The opinions or views stated in this article are those of its authors.

Appendix A. Supporting information

Supplementary data associated with this article can be found in the online version at doi:10.1016/j.jece.2023.109803.

References

[1] O. Al-sareji, M. Meiczinger, J.M. Salman, R.A. Al-Juboori, K.S. Hashim, V. Somogyi, M. Jakab, Ketoprofen and aspirin removal by laccase immobilized on date stones, Chemosphere 311 (Part 2) (2023), 137133, https://doi.org/10.1016/j.chemosphere.2022.137133.
[2] AquaSorb® CT, granular coconut shell based activated carbon, http://www.aquapuredepot.com/img/product/description/aquasorb%20ct.pdf.
[3] L. Arregui, M. Ayala, X. Gómez-Gil, G. Gutiérrez-Soto, C.E. Hernández-Luna, M. Herrera de Los Santos, L. Levin, A. Rojo-Domínguez, D. Romero-Martínez, M. C. Saparrat, M.A. Trujillo-Roldán, Laccases: structure, function, and potential application in water bioremediation, Microb. Cell Factor. 18 (1) (2019) 1–33.
[4] G.S.D.S. Barbosa, M.E.P. Oliveira, A.B.S. Dos Santos, O.C. Sánchez, C.M.F. Soares, A.T. Fricks, Immobilization of low-cost alternative vegetable peroxidase (Raphanus sativus L. peroxidase): choice of support/technique and characterization, Molecules 25 (16) (2020) 3668.
[5] M. Bilal, H.M. Iqbal, Sustainable bioconversion of food waste into high-value products by immobilized enzymes to meet bio-economy challenges and opportunities–A review, Food Res. Int. 123 (2019) 226–240.
[6] H.P. Boehm, Some aspects of the surface chemistry of carbon blacks and other carbons, Carbon 32 (5) (1994) 759–769.
[7] H. Cabana, C. Alexandre, S.N. Agathos, J.P. Jones, Immobilization of laccase from the white rot fungus Coriolopsis polyzona and use of the immobilized biocatalyst for the continuous elimination of endocrine disrupting chemicals, Bioresour. Technol. 100 (14) (2009) 3447–3458.
[8] R. Chong-Cerda, L. Levin, R. Castro-Ríos, C.E. Hernández-Luna, A. González-Horta, G. Gutiérrez-Soto, A. Chávez-Montes, Nanoencapsulated laccases obtained by double-emulsion technique. Effects on enzyme activity pH-dependence and stability, Catalysts 10 (9) (2020) 1085.

[9] R.O. Cristóvão, S.C. Silvério, A.P. Tavares, A.I.S. Brígida, J.M. Loureiro, R. A. Boaventura, E.A. Macedo, M.A.Z. Coelho, Green coconut fiber: a novel carrier for the immobilization of commercial laccase by covalent attachment for textile dyes decolourization, World J. Microbiol. Biotechnol. 28 (9) (2012) 2827–2838.
[10] Carlos Garca-Delgado, et al., Degradation of tetracyclines and sulfonamides by stevensite-and biochar-immobilized laccase systems and impact on residual antibiotic activity, J. Chem. Technol. Biotechnol. 93 (12) (2018) 3394–3409.
[11] M. Ghaedi, K. Mortazavi, M. Montazerozohori, A. Shokrollahi, M. Soylak, Flame atomic absorption spectrometric (FAAS) determination of copper, iron and zinc in food samples after solid-phase extraction on Schiff base-modified duolite XAD 761, Materials Science and Engineering: C 33 (4) (2013) 2338–2344.
[12] P. Ghosh, U. Ghosh, Immobilization of purified fungal laccase on cost effective green coconut fiber and study of its physical and kinetic characteristics in both free and immobilized form, Curr. Biotechnol. 8 (1) (2019) 3–14.
[13] L. He, Y. Yang, J. Kim, L. Yao, X. Dong, T. Li, Y. Piao, Multi-layered enzyme coating on highly conductive magnetic biochar nanoparticles for bisphenol A sensing in water, Chem. Eng. J. 384 (2020), 123276.
[14] J. Hu, B. Yuan, Y. Zhang, M. Guo, Immobilization of laccase on magnetic silica nanoparticles and its application in the oxidation of guaiacol, a phenolic lignin model compound, RSC Adv. 5 (120) (2015) 99439–99447.
[15] A. Imam, S.K. Suman, R. Singh, B.P. Vempatapu, A. Ray, P.K. Kanaujia, Application of laccase immobilized rice straw biochar for anthracene degradation, Environ. Pollut. 268 (2021), 115827.
[16] IRIMEX, Silcarbon K124, https://www.irimex.ru/services/catalog/aktivirovannye_ugli_i_katalizatoriy/silcarbon/silcarbon_k124/.
[17] A.H. Khan, H.A. Aziz, N.A. Khan, M.A. Hasan, S. Ahmed, I.H. Farooqi, A. Dhingra, V. Vambol, F. Changani, M. Yousefi, S. Islam, Impact, disease outbreak and the eco-hazards associated with pharmaceutical residues: a critical review, Int. J. Environ. Sci. Technol. (2021) 1–12.
[18] L. Lonappan, Y. Liu, T. Rouissi, S.K. Brar, R.Y. Surampalli, Development of biochar-based green functional materials using organic acids for environmental applications, J. Clean. Prod. 244 (2020), 118841.
[19] L. Lonappan, Y. Liu, T. Rouissi, S.K. Brar, M. Verma, R.Y. Surampalli, Adsorptive immobilization of agro-industrially produced crude laccase on various micro-biochars and degradation of diclofenac, Sci. Total Environ. 640 (2018) 1251–1258.
[20] Loos, R., Marinov, D., Sanseverino, I., Napierska, D. and Lettieri, T., Review of the 1st Watch List under the Water Framework Directive and recommendations for the 2nd Watch List, EUR 29173 EN, Publications Office of the European Union, Luxembourg, 2018, ISBN 978–92-79–81838-7 (print),978–92-79–81839-4 (pdf), doi:10.2760/614367 (online),10.2760/701879 (print), JRC111198.
[21] M. Naghdi, M. Taheran, S.K. Brar, A. Kermanshahi-Pour, M. Verma, R. Y. Surampalli, Immobilized laccase on oxygen functionalized nanobiochars through mineral acids treatment for removal of carbamazepine, Sci. Total Environ. 584 (2017) 393–401.
[22] M. Naghdi, M. Taheran, S.K. Brar, A. Kermanshahi-Pour, M. Verma, R. Y. Surampalli, Fabrication of nanobiocatalyst using encapsulated laccase onto chitosan-nanobiochar composite, Int. J. Biol. Macromol. 124 (2019) 530–536.
[23] E.F. Nájera-Martínez, E.M. Melchor-Martínez, J.E. Sosa-Hernández, L.N. Levin, R. Parra-Saldívar, H.M. Iqbal, Lignocellulosic residues as supports for enzyme immobilization, and biocatalysts with potential applications, Int. J. Biol. Macromol. (2022).
[24] D. Pandey, A. Daverey, K. Dutta, K. Arunachalam, Bioremoval of toxic malachite green from water through simultaneous decolorization and degradation using laccase immobilized biochar, Chemosphere 297 (2022), 134126.
[25] F.M. Putrino, M. Tedesco, R.B. Bodini, A.L. de Oliveira, Study of supercritical carbon dioxide pretreatment processes on green coconut fiber to enhance enzymatic hydrolysis of cellulose, Bioresour. Technol. 309 (2020), 123387.
[26] P. Rao, V. Rathod, Valorization of food and agricultural waste: a step towards greener future, Chem. Rec. 19 (9) (2019) 1858–1871.
[27] T. Rasheed, M. Bilal, F. Nabeel, M. Adeel, H.M. Iqbal, Environmentally-related contaminants of high concern: potential sources and analytical modalities for detection, quantification, and treatment, Environ. Int. 122 (2019) 52–66.
[28] B.S. Rathi, P.S. Kumar, D.V.N. Vo, Critical review on hazardous pollutants in water environment: occurrence, monitoring, fate, removal technologies and risk assessment, Sci. Total Environ. 797 (2021), 149134.
[29] A. Rehman, M. Park, S.J. Park, Current progress on the surface chemical modification of carbonaceous materials, Coatings 9 (2) (2019) 103.
[30] S. Rouhani, S. Azizi, R.W. Kibechu, B.B. Mamba, T.A. Msagati, Laccase Immobilized Fe3o4-Graphene Oxide nanobiocatalyst improves stability and immobilization efficiency in the green preparation of sulfa drugs, Catalysts 10 (4) (2020) 459.
[31] A. Samui, S.K. Sahu, One-pot synthesis of microporous nanoscale metal organic frameworks conjugated with laccase as a promising biocatalyst, N. J. Chem. 42 (6) (2018) 4192–4200.
[32] R.L. Singh, P.K. Singh, R.P. Singh, Enzymatic decolorization and degradation of azo dyes–a review, Int. Biodeterior. Biodegrad. 104 (2015) 21–31.
[33] T.M. de Souza Bezerra, J.C. Bassan, V.T. de Oliveira Santos, A. Ferraz, R. Monti, Covalent immobilization of laccase in green coconut fiber and use in clarification of apple juice, Process Biochem. 50 (3) (2015) 417–423.
[34] D. Spinelli, E. Fatarella, Di Michele, R. Pogni, R. Pogni, Immobilization of fungal (Trametes versicolor) laccase onto Amberlite IR-120 H beads: optimization and characterization, Process Biochemistry 48 (2) (2013) 218–223.
[35] STATISTA (2020) Coconut production worldwide from 2000 to 2020. https://www.statista.com/statistics/577497/world-coconutproduction/. (Accessed 10 October 2022).
[36] C.A. Toles, W.E. Marshall, M.M. Johns, Surface functional groups on acid-activated nutshell carbons, Carbon 37 (8) (1999) 1207–1214.
[37] P.D. Tomke, V.K. Rathod, A novel step towards immobilization of biocatalyst using agro waste and its application for ester synthesis, Int. J. Biol. Macromol. 117 (2018) 366–376.
[38] P. Tufvesson, W. Fu, J.S. Jensen, J.M. Woodley, Process considerations for the scale-up and implementation of biocatalysis, Food Bioprod. Process. 88 (1) (2010) 3–11.
[39] M. Valdez-Carrillo, L. Abrell, J. Ramírez-Hernández, J.A. Reyes-López, C. Carreón-Diazconti, Pharmaceuticals as emerging contaminants in the aquatic environment of Latin America: a review, Environ. Sci. Pollut. Res. 27 (36) (2020) 44863–44891.
[40] B. Varga, V. Somogyi, M. Meiczinger, N. Kováts, E. Domokos, Enzymatic treatment and subsequent toxicity of organic micropollutants using oxidoreductases-a review, J. Clean. Prod. 221 (2019) 306–322.
[41] A. Varghese, J. Jacob, A study of physical and mechanical properties of the Indian coconut for efficient dehusking, J. Nat. Fibers 14 (3) (2017) 390–399.
[42] R.A. Wahab, N. Elias, F. Abdullah, S.K. Ghoshal, On the taught new tricks of enzymes immobilization: an all-inclusive overview, React. Funct. Polym. 152 (2020), 104613.
[43] F. Wang, C. Guo, H.Z. Liu, C.Z. Liu, Immobilization of Pycnoporus sanguineus laccase by metal affinity adsorption on magnetic chelator particles, J. Chem. Technol. Biotechnol.: Int. Res. Process, Environ. Clean. Technol. 83 (1) (2008) 97–104.
[44] Z. Wang, Y. Zhang, K. Li, Z. Sun, J. Wang, Enhanced mineralization of reactive brilliant red X-3B by UV driven photocatalytic membrane contact ozonation, J. Hazard. Mater. 391 (2020), 122194.
[45] Z. Wang, D. Ren, S. Jiang, H. Yu, Y. Cheng, S. Zhang, X. Zhang, W. Chen, The study of laccase immobilization optimization and stability improvement on CTAB-KOH modified biochar, BMC Biotechnol. 21 (1) (2021) 1–13.
[46] X. Yao, L. Ji, J. Guo, S. Ge, W. Lu, L. Cai, Y. Wang, W. Song, H. Zhang, Magnetic activated biochar nanocomposites derived from wakame and its application in methylene blue adsorption, Bioresource technology 302 (2020) 122842.
[47] G.G. Ying, J.L. Zhao, L.J. Zhou, S. Liu, Fate and occurrence of pharmaceuticals in the aquatic environment (surface water and sediment), in: Comprehensive analytical chemistry, Vol. 62, Elsevier, 2013, pp. 453–557.
[48] J. Zdarta, A.S. Meyer, T. Jesionowski, M. Pinelo, Multi-faceted strategy based on enzyme immobilization with reactant adsorption and membrane technology for biocatalytic removal of pollutants: a critical review, Biotechnol. Adv. 37 (7) (2019), 107401.
[49] P. Zhang, Q. Wang, J. Zhang, G. Li, Q. Wei, Preparation of amidoxime-modified polyacrylonitrile nanofibers immobilized with laccase for dye degradation, Fibers Polym. 15 (1) (2014) 30–34.
[50] Y. Zhang, S.U. Geißen, C. Gal, Carbamazepine and diclofenac: removal in wastewater treatment plants and occurrence in water bodies, Chemosphere 73 (8) (2008) 1151–1161.
[51] Y. Zhang, M. Piao, L. He, L. Yao, T. Piao, Z. Liu, Y. Piao, Immobilization of laccase on magnetically separable biochar for highly efficient removal of bisphenol A in water, RSC Adv. 10 (8) (2020) 4795–4804.
[52] W. Zhou, W. Zhang, Y. Cai, Enzyme-enhanced adsorption of laccase immobilized graphene oxide for micro-pollutant removal, Sep. Purif. Technol. 294 (2022), 121178.